

Comparison of two routing metrics in OLSR on a grid based mesh network

David Johnson

Department of Electrical, Electronic and
Computer Engineering, University of Pretoria
Meraka Institute, CSIR
Pretoria, South Africa
Email: djohnson@csir.co.za

Gerhard Hancke

Department of Electrical, Electronic and
Computer Engineering, University of Pretoria
Pretoria, South Africa
Email: g.hancke@ieee.org

Abstract—Predicting the performance of ad hoc networking protocols for mesh networks has typically been performed by making use of software based simulation tools. Experimental study and validation of such predictions is a vital to obtaining more realistic results, but may not be possible under the constrained environment of network simulators. This paper presents an experimental comparison of OLSR using the standard hysteresis routing metric and the ETX metric in a 7 by 7 grid of closely spaced Wi-Fi nodes to obtain more realistic results. The wireless grid is first modelled to extract its ability to emulate a real world multi-hop ad hoc network. This is followed by a detailed analysis of OLSR in terms of hop count, routing traffic overhead, throughput, delay, packet loss and route flapping in the wireless grid using the hysteresis and ETX routing metric. It was discovered that the ETX metric which has been extensively used in mesh networks around the world is fundamentally flawed when estimating optimal routes in real mesh networks and that the less sophisticated hysteresis metric shows better performance in large dense mesh networks.

I. INTRODUCTION

Mesh networking is a relatively new technology originating out of ad hoc networking research from the early 90's. As a consequence, it is still thwart with many research challenges such as limited scalability, difficulty in choosing an appropriate routing protocol and lack of suitability to real time media traffic.

Traditionally ad hoc and mesh networking research has mostly been carried out using simulation tools but many recent studies [1] have revealed the inherent limitations these have in modelling the physical layer and aspects of the MAC layer. Researchers should acknowledge that the results from a simulation tool only give a rough estimate of performance. There is also a lack of consistency between the results of the same protocol being run on different simulation packages which makes it difficult to know which simulation package to believe.

Mathematical models are useful in the interpretation of the effects of various network parameters on performance. For example, Gupta and Kumar [2] have created an equation which models the best and worst case data rate in a network with shared channel access, as the number of hops increases. However, recent work done by the same authors [3] using a real test bed, employing laptops equipped with IEEE 802.11

Standard (802.11) based radios, revealed that 802.11 multi hop throughput is still far from even the worst case theoretical data rate predictions.

A recent Network Test Beds workshop report [4] highlighted the importance of physical wireless test bed facilities for the research community in view of the limitations of available simulation methodologies. This was the motivation for the ORBIT project [5] at Rutgers University and the Kansei testbed [6] at Ohio state University, that are the most comparable in design to the indoor testbed that was constructed as part of this work.

The ORBIT mesh lab consists of a 20x20 grid, which makes use of 802.11 wireless equipment based on the same Atheros chipset used in the Meraka lab. The ORBIT laboratory makes use of Additive White Gaussian Noise (AWGN) to raise the noise floor, while Meraka makes use of attenuators. The Kansei testbed consists of a 15 by 14 grid with nodes spaced 900 mm apart making use of 20 dB fixed attenuators to decrease the transmission range between the nodes.

These mini scale wireless grids can emulate real world physical networks due to the inverse square law of radio propagation, by which the electric field strength will be attenuated by 6.02 dB for each doubling of the distance.

The Optimized Link State Routing (OLSR) protocol [7] has been extensively used around the world for building low cost community owned mesh networks. These have mostly been located in urban areas but some have also been installed in rural areas, for example the Meraka Institute's Peebles Valley mesh project has managed to create a 9 node mesh network which connects schools, businesses and clinic infrastructure to a VSAT Internet link [8].

The Expected Transmission Rate (ETX) path metric, developed out of the MIT roofnet project [9], is a simple routing path metric that favors high-capacity, reliable links. The ETX metric is found from the proportion of beacons sent but not received in both directions on a wireless link. This metric has also been integrated into the OLSR routing protocol and a user now has a choice to either use the standard hysteresis routing metric or ETX.

This paper aims to report on 2 objectives:

- Show how an indoor network testbed based on a grid

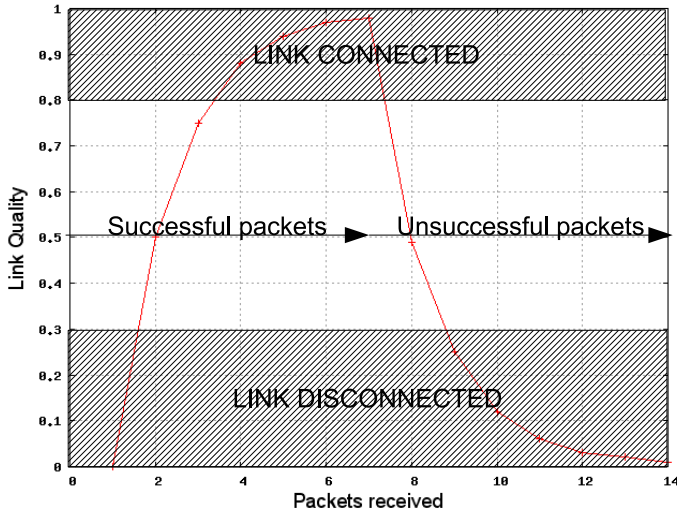


Fig. 2. Link Hysteresis in the OLSR routing protocol

The link quality, LQ , is the fraction of successful packets that were received by us from a neighbor within a window period. The neighbor link quality, NLQ , is the fraction of successful packets that were received by a neighbor node from us within a window period. Based on this, the ETX is calculated as follows:

$$ETX = \frac{1}{LQ \times NLQ} \quad (3)$$

In a multi-hop link the ETX values of each hop are added together to calculate the ETX for the complete link including all the hops. Figure 3 shows the ETX values for 7 consecutive successful packets followed by 7 consecutive unsuccessful packets assuming a perfectly symmetrical link and a link quality window size of 7.

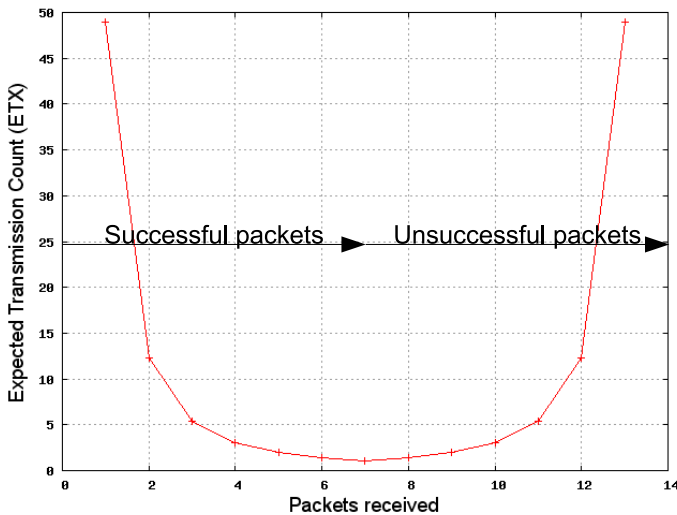


Fig. 3. ETX Path metric values for successive successful and unsuccessful packets

A perfect link is achieved when ETX is equal to 1. ETX has

the added advantage of being able to account for asymmetry in a link as it calculates the quality of the link in both directions. Unlike Hysteresis ETX improves and degrades at the same rate when successful and unsuccessful packets are received respectively. Routes are always chosen such that the sum of all the ETX values of adjacent node pairs is minimized.

C. Linux Implementation of ad-hoc networking protocols

A crucial part of comparing a different ad hoc networking protocols on a real testbed is finding implementations of the protocol that are well written and are as close as possible to the original published RFC.

The choice between a multitude of implementations of the same protocol was based on whether the particular implementation claimed to be RFC compliant, and if there was a strong developer community supporting the code base. Preference was also given to cases where the same code base was used for simulations and running the code on a physical network as this would make future comparisons of simulations and live network results very simple.

For OLSR, the implementation developed by Tonnesen [12] was used. This implementation is commonly called olsr.org and is now part of the largest open source ad hoc networking development initiative. Version 0.4.10, which is RFC3626 compliant, is used and is capable of using the standard RFC link hysteresis metric or the new ETX metric for calculating optimal routes. All parameters mentioned in the RFC are implemented and can be modified through a configuration file.

III. CONSTRUCTION OF THE MESH TESTBED

The mesh testbed consists of a wireless 7x7 grid of 49 nodes, which was built in a 6x12 m room as shown in Figure 4. A grid was chosen as the logical topology of the wireless testbed due to its ability to create a fully connected dense mesh network and the possibility of creating a large variety of other topologies by selectively switching on particular nodes as shown in Figure 5.

Each node in the mesh consists of a VIA 800 C3 800MHz motherboard with 128MB of RAM and a Wistron CM9 mini PCI Atheros 5213 based Wi-Fi card with 802.11 a/b/g capability. For future mobility measurements, a Lego Mindstorms robot with a battery powered Soekris motherboard containing an 802.11a (5.8 GHz) WNIC and an 802.11 b/g (2.4 GHz) WNIC shown in Figure 4 can be used.

Every node was connected to a 100 Mbit back haul Ethernet network through a switch to a central server, as shown in Figure 6. This allows nodes to use a combination of a Pre-boot Execution Environment (PXE), built into most BIOS firmware, to boot the kernel and a Network File System (NFS) to load the file system.

The physical constraints of the room, with the shortest length being 7m, means that the grid spacing needs to be about 800 mm to comfortably fit all the PCs within the room dimensions.

At each node, an antenna with 5 dBi gain is connected to the wireless network adapter via a 30 dB attenuator. This

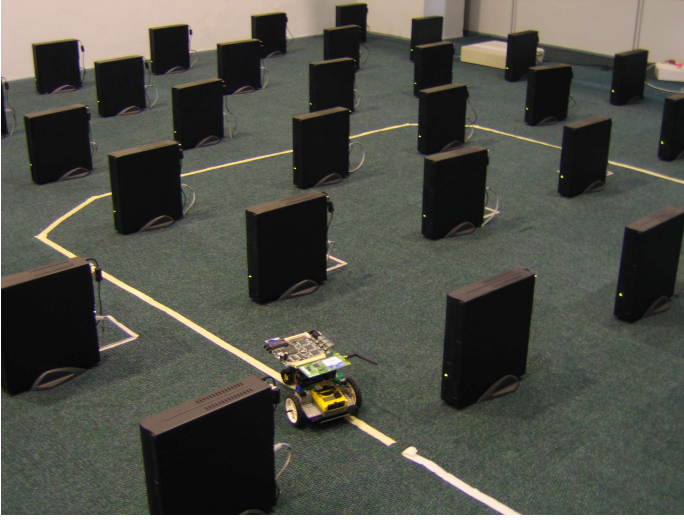


Fig. 4. Layout of the 7x7 grid of Wi-Fi enabled computers, the line following robot is an option, which will be explored in the future to test mobility in a mesh network.

introduces a path loss of 60 dB between the sending node and the receiving node. Reducing the radio signal to force a multi hop environment, is the core to the success of this wireless grid and this is discussed later.

The wireless NICs that are used in this grid have a wide range of options that can be configured:

- *Power level range:* The output power level can be set from 0 dBm up to 19 dBm.
- *Protocol modes:* 802.11g and 802.11b modes are available in the 2.4 GHz range and 802.11a modes are available in the 5 GHz range
- *Sending rates:* 802.11b allows the sending rate to be set between 1 Mbps and 11 Mbps and 802.11g allows between 6 Mbps and 54 Mbps

This network was operated at 2.4 GHz due to the availability of antennas and attenuators at that frequency, but in future the laboratory will be migrated to the 5 GHz range, which has many more available channels with a far lower probability of being affected by interference.

IV. ELECTROMAGNETIC MODELING

In order to check if nodes in the wireless grid can be limited to only communicate over short distances and force the creation of a multi-hop environment, the radio environment is now examined. The receive sensitivity of the radio, which is the level above which it is able to successfully decode a transmission, depends on the mode and data rate being set. The faster the rate, the lower the receive sensitivity threshold.

Figure 7 shows free space loss curves for all possible scenarios over the distance of the grid to illustrate what the received signal will be at any particular node. This figure also shows the receive sensitivity of the radio at various modes and data rates. In theory, where the curve line rises above the horizontal lines, there will be connectivity but as will be seen

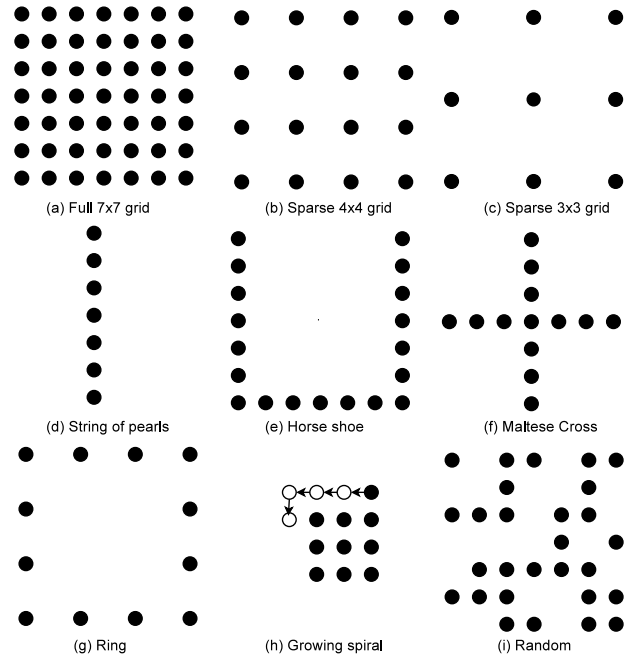


Fig. 5. Various topologies that can be tested on the 7x7 grid; diagrams (a) to (c) demonstrate various levels of density in a grid; diagram (e) is used to create a long chain to force routing protocols to use the longest multi-hop route, and diagram (g) is used to test route optimization.

later, there are factors other than free space loss which affect signal propagation.

The minimum possible range is 150 mm when the radios are set to 802.11g mode, a data rate of 54 Mbps and a transmit power level of 0 dBm. This would prevent any connectivity between nodes in the grid which are space at 800mm. The maximum possible range is 17.26 m when the radios are set to 802.11b mode, a data rate of 1 Mbps and a transmit power level of 20 dBm. This would enable all 49 nodes in the grid to communicate with each other. It is clear from this that a good range of connectivity density can be created by adjusting the parameters on the radios.

Signal measurements between 10584 random node pairs in the 7x7 grid were recorded to compare measured and predicted free space loss signal strength versus distance in Figure 8. The discrete distances that are apparent for the measured signal are due to the finite number of possible distances in a 7x7 grid for all possible links between each node.

There is a general trend for the measured signal strength to become weaker than the predicted free space loss signal strength as the distance increases. This is most likely due to the effect of Fresnel zone interference shown in Figure 9 The large 10dB standard deviation for measurements made with the same distance is due to multipath fading and other issues such as antenna coupling. Overall the result shows a decay pattern which matches the predicted free space loss fairly well.

Antenna coupling occurs when antenna antennas are placed in close proximity to each other and they form a complex propagation path as each antenna re-transmits some of the re-

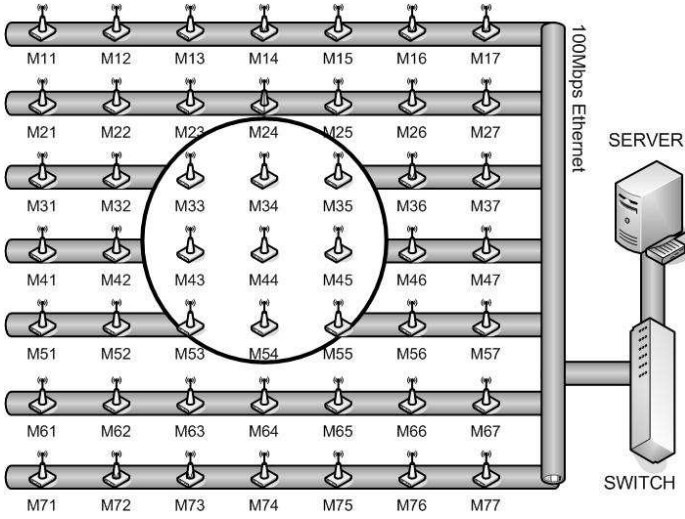


Fig. 6. The architecture of the mesh lab. Ethernet is used as a back channel to connect all the nodes to a central server through a switch. Each node is also equipped with an 802.11 network interface card.

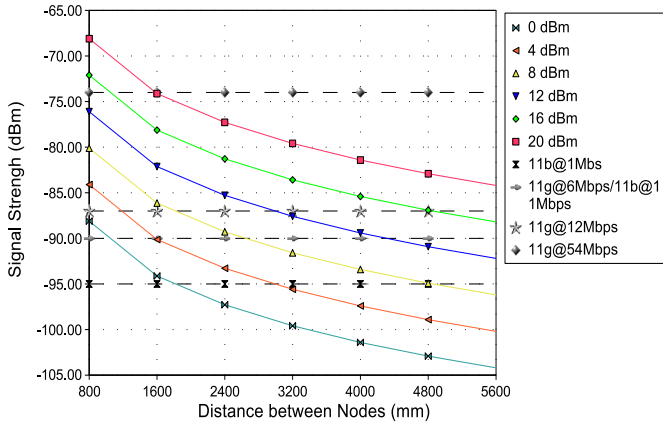


Fig. 7. Received signal strength vs. distance between nodes in the grid spaced 800 mm apart. The horizontal lines show the receive sensitivity of the Atheros 5213 wireless network card. If the received signal strength curve is above this line, there will be connectivity between the nodes.

ceived signal. These antennas form an array which effectively changes the effective radiation pattern of the transmitter from the point of view of the receiver. The antenna gain pattern is calculated as a product of the antennas own pattern and an array factor which is determined by the geometry of the array. Antenna coupling can cause deviation as high as 7 dB.

V. ESTABLISHING A BASELINE FOR THE MEASUREMENTS

In order to establish the baseline for performance of the wireless nodes in the grid, it is useful to remove any effects of routing and establish the best possible multi-hop throughput and delay between the nodes. Figure 10 shows a string of pearls 49 nodes long built by creating a zigzag topology in the grid, using manually configured static routes.

All the radios were set to their maximum power (20 dBm),

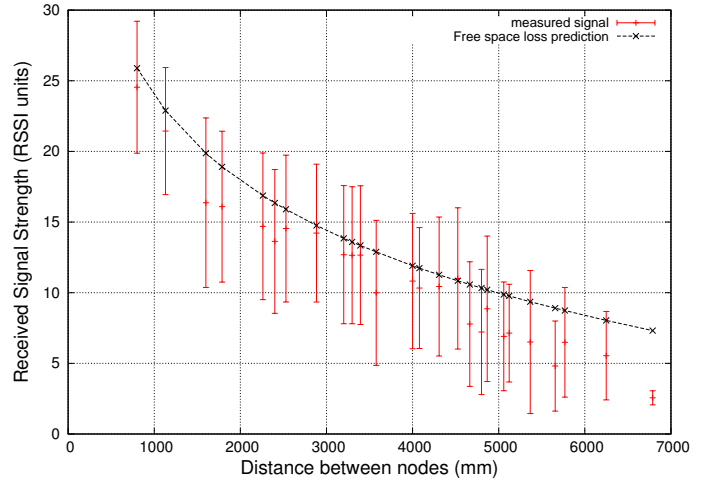


Fig. 8. Comparison between measured and predicted free space loss received signal strength

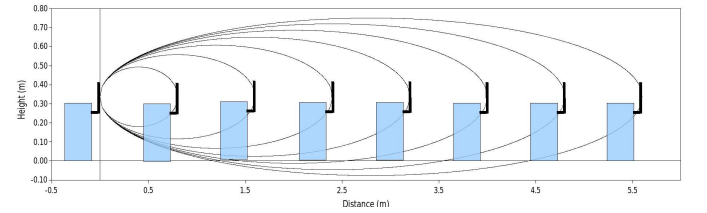


Fig. 9. 1st Fresnel zone obstruction between column of 7 PCs

using 802.11b mode with a data rate of 11 Mbps to avoid any packet loss. Throughput degradation due to hop count in packet based networks with single radios has been well studied by Gupta *et al* [2]. The theoretical best case and worst case throughput in an asymptotic sense is given by Equations 4 and 5.

$$\lambda_{WORST}(n) = \frac{W}{\sqrt{n \log(n)}} \quad (4)$$

$$\lambda_{BEST}(n) = \frac{W}{\sqrt{n}} \quad (5)$$

where W = Bandwidth of first hop and n = number of hops.

These equations do not take into account effects of the 802.11 MAC layer protocol or signal propagation and, as such, present an idealistic case only valid in an asymptotic sense. A recent study [3] by the Gupta and Kumar using laptops equipped with 802.11 based radios placed in offices revealed, using a least-squares fit, that the actual data rate versus the number of hops is given by Equation 5.

$$\lambda_{GUPTA_{LMS}}(n) = \frac{W}{n^{1.68}} \quad (6)$$

This represents a dramatic difference in throughput after a multiple number of hops for 802.11 compared to the theoretical predictions. After 10 hops the measured results differed

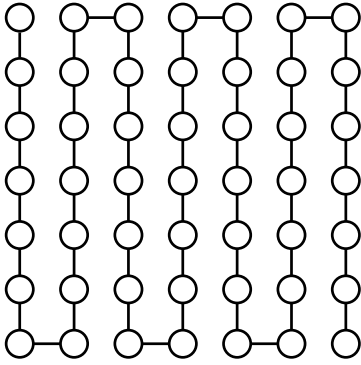


Fig. 10. Creation of a string of pearls topology 49 nodes long using the 7x7 grid.

by as much as 10% compared to the theoretical worst-case prediction.

Throughput and delay measurements were now carried out on the 7x7 grid using the mechanisms highlighted in Section VII.

Figure 11 shows the results of these multi-hop throughput measurements and compares them to theoretical and previously measured results. The measurements revealed a less pessimistic result but one which was still less than the worst-case theoretical predictions. The asymptotic validity of Gupta's theoretical predictions is clearly shown for small hop counts where after 2 hops, the worst case prediction is actually higher than the best case prediction.

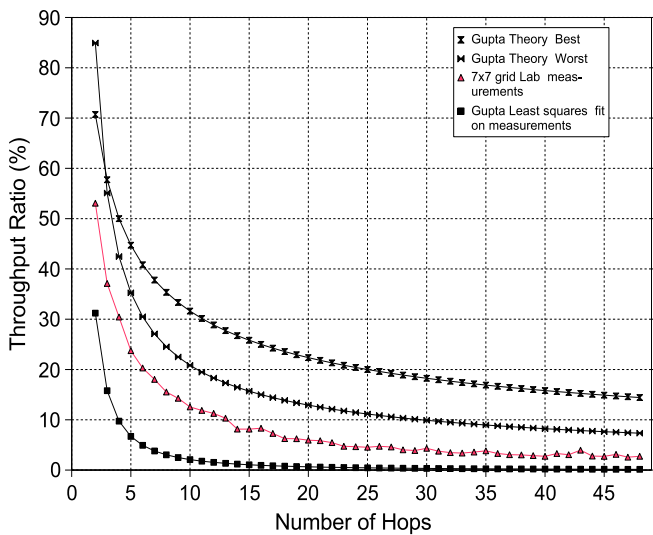


Fig. 11. Comparison of 7x7 grid multi hop throughput to theoretical and other measured results.

Carrying out a least squares fit on the results obtained with the testbed, and using a plot of the log of both the x and y-axis as shown in Figure 12 reveals the following function for TCP

throughput under ideal conditions for the grid.

$$\lambda_{LMSGRID}(n) = \frac{W}{n^{0.98}} \quad (7)$$

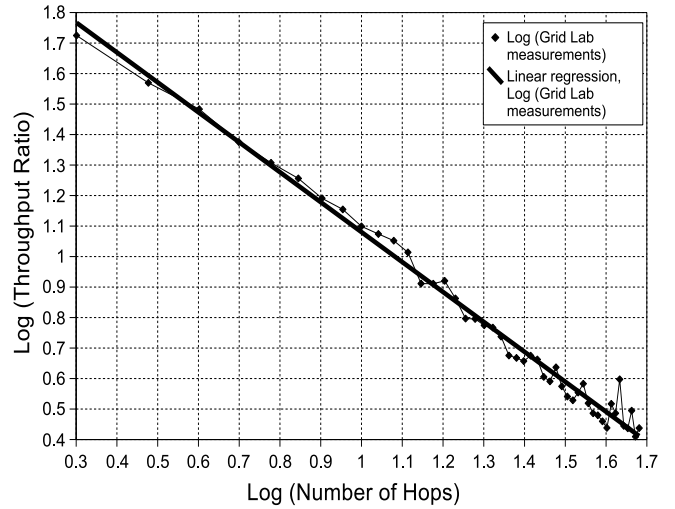


Fig. 12. Linear regression of log of the throughput vs the log of the hop count for 49 node long chain in 7x7 grid

VI. MODELLING THE COMPLEXITY OF THE GRID

The higher the degree of connectivity between nodes in the grid, the more complex the routing decision becomes for an ad hoc routing algorithm. The number of edges leaving or entering a vertex gives a good indication of the complexity within a graph. If the signal strength is higher, the degree of connectivity within the grid will increase. Although this will potentially decrease the hop count across the grid, it has many other negative outcomes. Firstly it increases the convergence time of the routing protocol, secondly it causes more interference amongst nodes in the grid and thirdly it has the potential to cause more route flapping between pairs of communicating nodes with certain routing protocols [15].

To illustrate this, Figure 13 shows all the possible connections between nodes for a 7x7 grid if the signal radius is in the range greater than or equal to $\sqrt{2}$ and less than 2 in a unit spaced grid where a path is sought from $A1$ to $G7$. Some boundary conditions were set which specify that a directed edge to a vertex can only be created if the vertex is closer to the destination than the previous vertex.

A recursive "path search" algorithm was developed to calculate all possible routes through the grid. The total number of routes possible in this graph is 170277. To illustrate the range of hop categories, there are 42 "2 hop" routes, 490 "3 hop routes" and 22320 "7 hop" routes through the grid for this radius.

To understand how the complexity of the grid changes as the coverage radius increases, the number equivalent hop routes is plotted in Figure 14 up to a total of 4 hops for a radius increasing from unit length up to the length of a diagonal

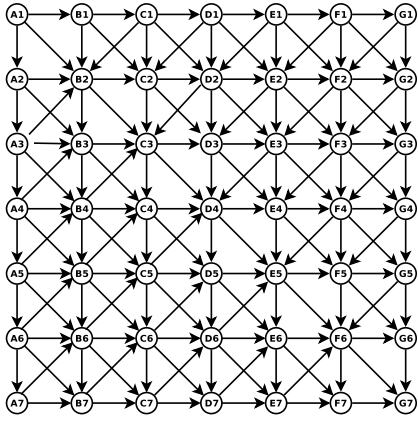


Fig. 13. All possible connections between nodes if signal radius is greater than or equal to $\sqrt{2}$ and less than 2 in a unit spaced grid and all vertices in a path decrease the distance to the destination

between the furthest two points on the grid which is $6\sqrt{2}$. The depth of the search was limited to 5 hops due to the search space being large for even a days computation time. These graphs follow a sigmoid curve with increasing signal radius.

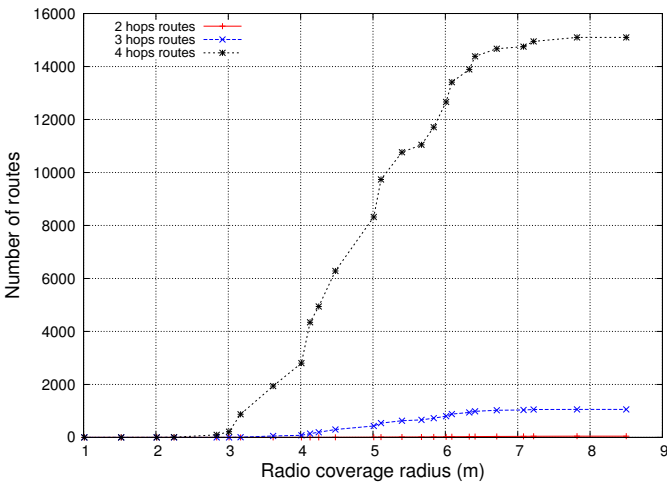


Fig. 14. Number of equivalent hops routes through a 7x7 unit spaced grid for a radius range of 1 to $6\sqrt{2}$

The larger the number of equivalent hop routes in a network, the harder it is for a hop count based routing algorithm to settle on an optimum route and if some damping isn't employed the algorithm will tend to flap between routes. A special case in point is where the radius is greater than or equal to 1 and less than $\sqrt{2}$. In this case there is only one hop count category of 12 hops with a total of 924 possible routes. This is the worst case scenario in terms of the number of shortest path routes to the destination.

VII. MEASUREMENT PROCESS

All measurements other than throughput tests were carried out using standard Unix tools available to users as part of the operating system. The measurement values were sent back to

the server via the Ethernet ports of the nodes and therefore had no influence on the experiments that were being run on the wireless interface.

It was found that the lab provides the best multi hop characteristics trade off with the best delay and throughput when the radios are configured with the following settings:

- Channel = 6
- Mode = 802.11b
- Data rate = 11 Mbps
- TX power = 0 dBm

In order to avoid communication gray zones [13], which are illustrated in Figure 15, the broadcast rate is locked to the data rate. Communication grey zones occur because a node can hear broadcast packets, as these are sent at very low data rates, but no data communication can occur back to the source node, as this occurs at a higher data rate.

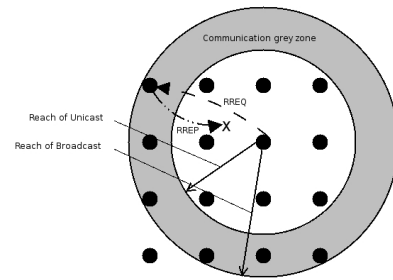


Fig. 15. Communication grey zones.

The following measurement processes were used for each of the metrics being measured in the ad hoc routing protocols:

- 1) *Delay*: Standard 84 byte ping packets were sent for a period of 10 seconds. The ping reports the round trip time as well as the standard deviation.
- 2) *Packet loss*: The ping tool also reports the amount of packet loss that occurred over the duration of the ping test
- 3) *Static Number of hops for a route to a destination*: The routing table reports the number of hops as a routing metric.
- 4) *Round trip route taken by a specific packet*: The ping tool has an option to record the round trip route taken by an ICMP packet but unfortunately the IP header is only large enough for nine routes. This sufficed for most of the tests that were done but occasionally there were some routes, which exceeded 9 round trip hops, and no knowledge of the full routing path could be extracted in these instances. However this was large enough to always record the forward route taken by a packet.
- 5) *Route flapping*: Using the ping tool with the option highlighted above to record the complete route taken by a packet every second, it is a simple process to detect how many route changes occurred during a set period of time by looking for changes in the route reports.

- 6) *Throughput*: The tool Iperf [16] was used for throughput measurements. It uses a client server model to determine the maximum bandwidth available in a link using a TCP throughput test but can also support UDP tests with packet loss and jitter. For these experiments an 8K read write buffer size was used and throughput tests were performed using TCP for 10 seconds. UDP could be considered a better choice as it measures the raw throughput of the link without the extra complexity of contention windows in TCP. This does make the measurement more complex, however, as no prior knowledge exists for the link and the decision on the test transmission speed is done through trial and error.
- 7) *Routing traffic overhead*: In order to observe routing traffic overhead the standard Unix packet sniffing tool tcpdump was used. A filter was used on the specific port that was being used by the routing protocol. The measurement time could be varied by the measurement script, but 20 seconds was the default that was mostly used. The tool made it possible to see the number of routing packets leaving and entering the nodes as well as the size of these routing packets. To force dynamic routing protocols such as AODV and DYMO to generate traffic while establishing a route, a ping was always carried out between the furthest two points in the network.
- 8) *Growing network size*: When tests are done which compare a specific feature to the growing number of nodes in the network, a growing spiral topology, shown in Figure 16, starting from the center of the grid, is used. This helps to create a balanced growth pattern in terms of distances to the edge walls and grid edges, which may have an electromagnetic effect on the nodes.

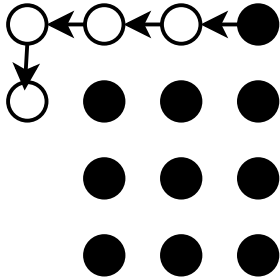


Fig. 16. Growing spiral topology for tests which compares a metric against a growing network size.

- 9) *Testing all node pairs in the network*: When throughput and delay tests were carried out on a fixed size topology, all possible combinations of nodes were tested. If the full 7x7 grid was used this equates to 2352 (49×48) combinations.
- 10) *RTS/CTS tuned off*: All tests are done with RTS/CTS disables as this did not improve the performance of the mesh, other researchers have reported similar findings [14]

VIII. RESULTS

Performance analysis of OLSR with two routing metrics is now presented. In all the graphs the term OLSR-RFC refers to OLSR making use of the default hysteresis routing metric defined in the RFC. OLSR-ETX refers to OLSR making use of the new ETX routing metric.

A. Hop count distribution

The ability to create a multi hop network in the mesh testbed is a key measure of the ability of the lab to emulate a real world wireless mesh network. From signal strength measurements in Section IV it was clear that the range of the signal can be limited to just under a meter. This section will now verify this from the perspective of the routing protocol creating a multi-hop topology.

In order to evaluate how the multi-hop environment evolves as the network grows, a growing spiral topology, as described in Section VII, was used. OLSR, using ETX as a routing metric, was chosen for the experiment as it has a built in “graphical topology representation” feature, which makes it easy to visually inspect how effectively the lab creates a multi-hop environment.

A node was added to the spiral every 10 seconds and the wireless NICs were configured to 802.11b mode, 11 Mbps data rate and a power level of 0 dBm. Figure 17 shows the total number of routes in specific hop categories versus a growing number of nodes in the grid. Up to 5 hop links were achieved with 2 hop links forming the dominant category after 16 nodes. This shows that a good spread of multi-hop links has been achieved in the grid.

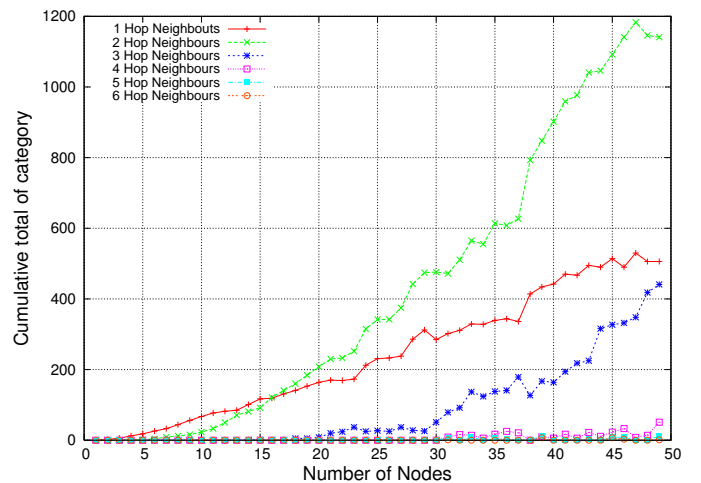


Fig. 17. Total number of routes in specific hop categories versus a growing number of nodes in the grid.

B. Routing overhead

The ability of a routing protocol to scale to large networks is highly dependent on its ability to control routing traffic overhead. Routing traffic contains messages that a routing protocol needs to establish new routes through a network, maintain

routes or repair broken routes. These can be simple HELLO messages which are sent periodically to allow neighbouring nodes to learn about the presence of fellow nodes or they can be topology messages containing routing tables.

The amount of inbound and outbound routing traffic as well as the packet size of routing packets was measured as the network size grows in a spiral fashion. The measurement process was described in Section VII. Once this data was collected for each node in the network, the traffic was averaged across all the nodes in the network and normalized to the amount of traffic per second.

Figure 18 shows the inbound traffic for all both routing metrics for OLSR and Figure 19 shows the outbound traffic. OLSR-ETX had slightly more routing traffic than OLSR-RFC as it made use of less hops. This becomes more pronounced as the number of nodes increase. When a routing protocol has less hops, the coverage of a single node's routing broadcast traffic is wider and adjacent nodes will be receiving and forwarding more routing traffic.

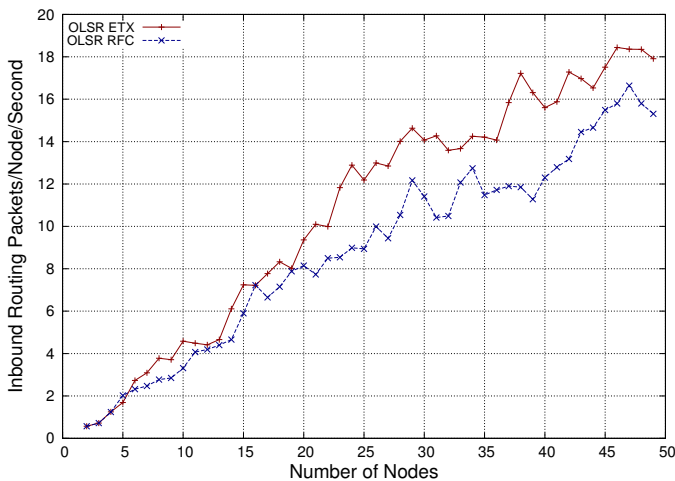


Fig. 18. Inbound routing packets per node per second versus increasing number of nodes using a growing spiral.

Figure 19 shows that the outbound traffic is less than the inbound traffic as the routing algorithm makes a decision to rebroadcast the packet or not. This shows that OLSR is making use of MPRs to limit the rebroadcast of route discovery or maintenance packets.

Figure 20 shows how routing packet lengths grow as the number of nodes increase. This is another important characteristic to analyze if a routing protocol is to scale to large networks. As the network grows, OLSR needs to send the entire route topology in Topology Control (TC) update messages, which helps explain this steady linear increase with the number of nodes. OLSR with the ETX extension uses a longer packet length due to the extra overhead of carrying link quality metrics.

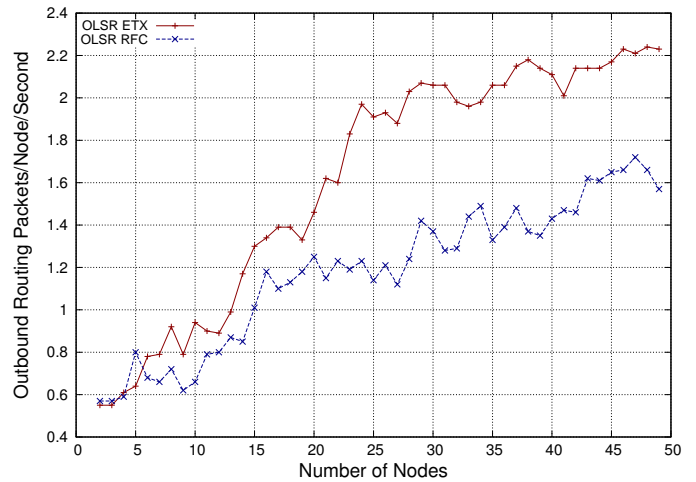


Fig. 19. Outbound routing packets per node per second versus increasing number of nodes using a growing spiral.

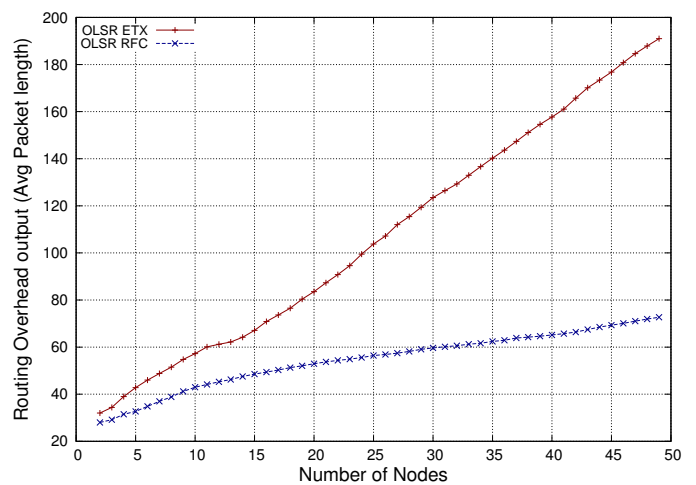


Fig. 20. Average Routing Packet length growth versus increasing number of nodes.

C. Throughput, packet loss, route flapping and delay measurements

The ability of a routing algorithm to find an optimal route in the grid will be exposed by its throughput, packet loss and delay measurements. Route flapping, which is an established phenomenon in wireless mesh networks [15], can also have a serious detrimental effect on the performance of the network.

The maximum network complexity was used to test which routing metric in OLSR performed the best under difficult conditions with thousands of alternative routes. Tests were carried out for all 2352 (49×48) possible pairs in the 7×7 grid and Table I highlights the averages for all the results.

OLSR using hysteresis (OLSR-RFC) was clearly the best performing protocol on all accounts from this table achieving an average of 11% better throughput, 3% less broken links and marginally less delay and packet loss. This was in spite of far higher route flapping (an average of 2.34 route flaps every 10 seconds compared to 0.25 for OLSR with ETX).

TABLE I

Comparison of throughput, delay and packet loss for full 7x7 grid

Routing Protocol	Forward hop count	Route changes	Packet loss (%)	Delay (ms)	Throughput (kbps)	No link (%)
OLSR-ETX	1.84	0.25	24.05	68.84	1187.57	19.2
OLSR-RFC	2.28	2.34	22.22	67.44	1330.05	16.2

Forward Hop count was also 67% higher than OLSR-ETX which showed that it was clearly selecting high quality short hop links over less hops with poorer quality links.

The following graphs take a closer look at how these protocols perform as the distance between the nodes increase.

A very clear relationship between route changes and distance is seen for the OLSR-RFC protocol in Figure 21, which increases fairly linearly and begins to level off after about 4 m.

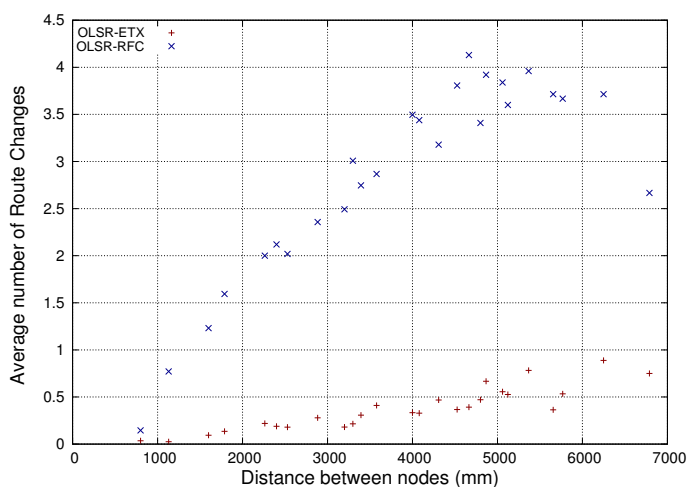


Fig. 21. Route changes versus distance for the OLSR protocol in the 7x7 wireless grid

Figure 22 shows the hop count for OLSR-RFC quickly diverging from OLSR-ETX as the distance increases. The higher the hop count the more alternative routes there are to choose from which will result in a higher degree of route flapping.

But clearly this route flapping, which occurred in OLSR-RFC has only had a positive effect on throughput, which means that the routing protocol was converging on more optimal routes rather than diverging from them. Figure 23 shows that OLSR-RFC is always slightly better than OLSR-ETX over the full range of the grid. The cumulative distribution function in Figure 24 shows that OLSR-RFC has a stronger distribution of links on the upper side of 2000 kbps than on the lower side. Whereas OLSR-ETX starts off with a greater number of failed links (40%) when running throughput tests and has a higher concentration of lower speed links.

The ETX routing metric [9] was developed to improve the performance of routing in static wireless mesh networks where hop count was not suitable. However OLSR-

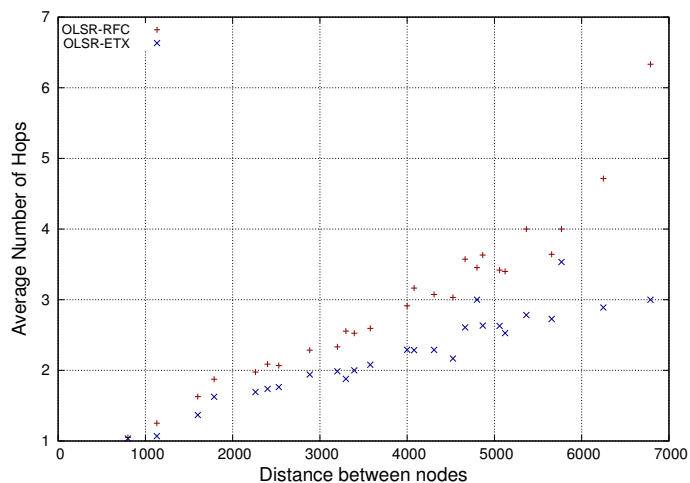


Fig. 22. hop count versus distance for the OLSR protocol in the 7x7 wireless grid

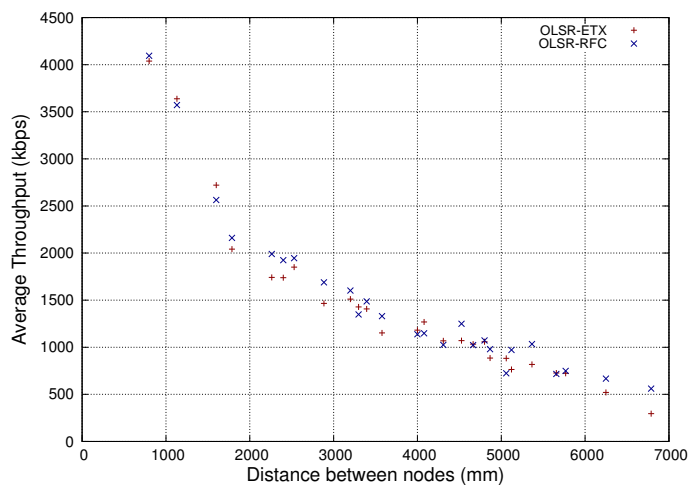


Fig. 23. Throughput versus distance for the OLSR protocol in the 7x7 wireless grid

ETX appeared to perform worse than OLSR-RFC overall, this could be because hysteresis is better at quickly converging on more optimal routes in a highly dense mesh like this indoor wireless grid as its condition for considering a link established is stricter than the condition for dropping a link. Further comparisons will be necessary to understand how mesh density and convergence time effect the results.

IX. COMPARISON OF THROUGHPUT RESULTS AGAINST BASELINE

Figure 25 shows how the routing protocols performance compared to the ideal multi hop network that was set up in Section V.

The baseline presents the best possible throughput the routing protocols could achieve in the indoor wireless grid. OLSR-RFC reaches the baseline for the first 3 hops and then begins to drop off the target after 4 hops. OLSR-ETX falls inbetween the baseline and Gupta's indoor measurements

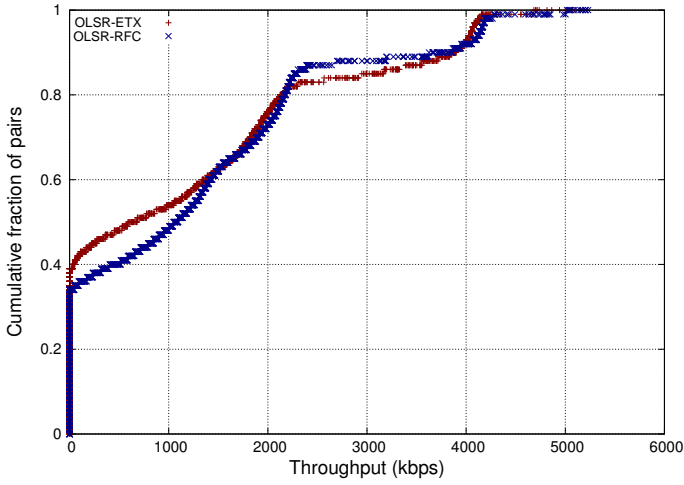


Fig. 24. Cumulative distribution function for the OLSR protocol in the 7x7 wireless grid

which are about 20% lower than the baseline measurement. This demonstrates that the conditions in the lab are far better than making use of offices to create a wireless testbed and relying on office walls to attenuate the signal.

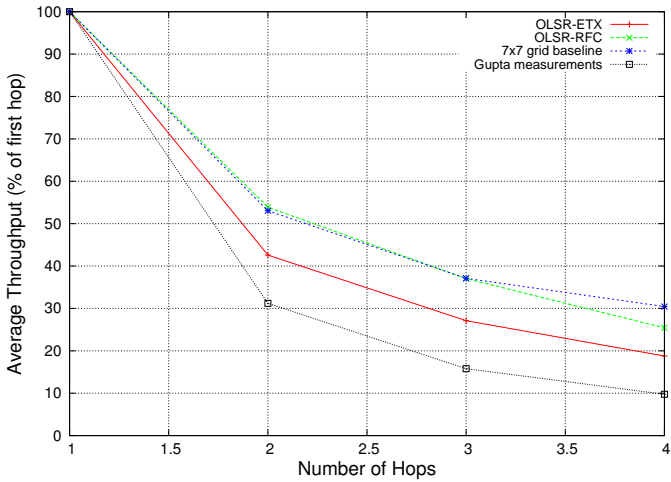


Fig. 25. Comparison of routing protocol throughput to baseline

X. A CHALLENGE TO THE ETX METRIC

The performance analysis that carried out so far has revealed that the ETX metric used with OLSR does not perform as well as using the standard hysteresis routing metric. This section will now revisit the ETX metric in real networks and calculate whether it accurately predicts whether a specific multi-hop path is optimal.

Consider a simple network shown in Figure 26

ETX values were calculated based on Equations 8 and 9

$$ETX = \frac{1}{LQ \times NLQ} \quad (8)$$

$$ETX'_{AD} = ETX_{AB} + ETX_{BC} + ETX_{CD} \quad (9)$$

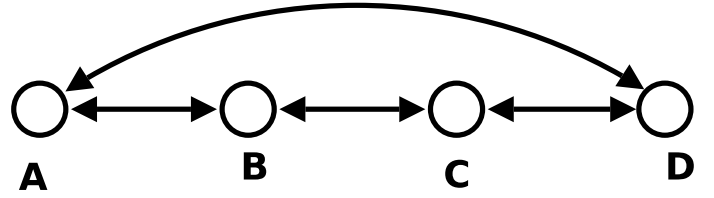


Fig. 26. Simple 4 node string of pearls topology with 1 hop and 3 hop routes

Two routes are possible in this graph between A and D; a single hop route denoted by ETX_{AD} and a 3-hop route denoted by ETX'_{AD} .

If the links were all perfectly symmetrical links with no packet losses then the following ETX values would be predicted for all the single hop paths from A to D shown in Equations 10 to 13. The multi hop ETX value for the path from A to D is shown in Equation 14.

$$ETX_{AB} = 1 \quad (10)$$

$$ETX_{BC} = 1 \quad (11)$$

$$ETX_{CD} = 1 \quad (12)$$

$$ETX_{AD} = 1 \quad (13)$$

$$ETX'_{AD} = 3 \quad (14)$$

Since ETX is a prediction of the average number of packet transmission required for a successful packet to arrive at its destination and vice versa, the throughput, in one direction, expressed as a fraction of the maximum achievable throughput, if all packets were successful, is the inverse square root of this.

$$\lambda'_{AD} = \frac{1}{\sqrt{ETX'_{AD}}} \quad (15)$$

Gupta's best case throughput prediction expressed as a fraction of the throughput of the first hop is given by Equation 16

$$\lambda_{BEST}(n) = \frac{1}{\sqrt{n}} \quad (16)$$

For perfectly symmetrical links with no packet loss these equations become equivalent and the prediction for throughput as a fraction of the first hop throughput is given by Equation 17.

$$\lambda'_{AD} = \lambda_{BEST}(n) = \frac{1}{\sqrt{3}} = 0.58 \quad (17)$$

But a model developed in ideal conditions in the mesh lab reveals a model for throughput given by Equation 18 :

$$\lambda_{LAB}(n) = \frac{1}{n^{0.98}} \quad (18)$$

Throughput expressed as a fraction of the first hop throughput after 3 hops in a live network with no losses is given by Equation 19:

$$\lambda_{LAB}(3) = \frac{1}{3^{0.98}} = 0.34 \quad (19)$$

This shows that the predicted losses using the ETX algorithm are out by a factor of almost 2 compared to the actual losses that will be experienced, even in ideal lab conditions for 802.11. Analysis of the results for this specific scenario shows that ETX will only calculate the correct routes with the following conditions: The percentage of successful packets for ETX_{AD} is less than 34%, in which case it will correctly choose the multi-hop route, ETX'_{AD} , the percentage of successful packets for ETX_{AD} is greater than 58%, in which case it will correctly choose the single-hop route, ETX_{AD} . Any value between 34% and 58% will result in ETX incorrectly choosing the multi-hop route, ETX'_{AD} .

If ETX was modified to correctly predict optimal routes in all circumstances, it would lead to routes with shorter hops being chosen. This seems counter intuitive, as OLSR with hysteresis performed better with a higher number of hops, but reveals that the optimal hop count search space consists of local maxima and there is not a single clear optimal average hop count.

In the future, a weighted ETX calculation could possibly be used which bases its weights on live network measurements to more accurately predict optimal paths over multi-hop links.

XI. CONCLUSION

The results from experiments done in the wireless grid lab have shown that it is possible to build a scaled wireless grid which yields good multi hop characteristics. Currently hop counts up to 5 are achievable with routing protocols in the full 7x7 grid when the power is set to 0dBm with 30 dB attenuators.

A grid structure does yield a worst-case complexity problem for routing protocols in terms of the number of alternative routes available between distant points in the grid. This has a severe impact on route flapping if some kind of damping is not employed.

Detailed analysis of OLSR with the hysteresis and ETX routing metric revealed that the original hysteresis metric performs better than ETX in a large dense mesh network. An analysis was then carried out on the ETX protocols which revealed that in realistic networks, the predicted losses using the ETX algorithm are out by a factor of almost 2 compared to the actual losses that will be experienced even in ideal lab conditions for 802.11.

XII. FUTURE CONSIDERATIONS

The current testbed forms a good baseline for future experimental research where the performance of new or improved ad hoc networking protocols can be analysed.

All these performance tests were carried out using suggested configuration parameters that are published in MANET RFCs

and Internet drafts, in the future it will be interesting to see how performance can be tweaked for specific topologies by changing parameters such as HELLO intervals.

These experiments were performed using a single data flow through the network between a pair of nodes being tested. In the future, the effect of multiple data flows on the routing, throughput or delay performance would be vital to establishing a complete picture of the network performance of routing protocols in a mesh network.

What has emerged out of this work is that simulation based results and results from real wireless networks are often very different. Further work on refining routing algorithms and routing metrics to adapt to live network conditions is now required.

REFERENCES

- [1] T.R. Andel and A. Yasinac, "On the credibility of manet simulations," *Computer*, vol. 39, no. 7, pp. 48–54, July 2006.
- [2] P. Gupta and P.R. Kumar, "The capacity of wireless networks," *IEEE Transactions on Information Theory*, vol. 46, no. 2, pp. 288–404, March 2000.
- [3] P. Gupta and R. Drag, "An experimental scaling law for ad-hoc networks," Tech. Rep., Bell Laboratories, 2006.
- [4] "Nsf workshop on network research testbeds, chicago, il," October 2002, http://www.net.cs.umass.edu/testbed_workshop/.
- [5] S. Ganu, H. Kremono, R. Howard, and I. Seskar, "Addressing repeatability in wireless experiments using the orbit testbed," in *Proceedings of IEEE Tridentcom*, Trento, Italy, February 2005.
- [6] V. Naik, E. Ertin, H. Zhang, and A. Arora, "Wireless Testbed Bonsai," *Proc. 2nd Intl Workshop Wireless Network Measurement*.
- [7] P. Jacquet, P. Muhlethaler, T. Clausen, A. Laouiti, A. Qayyum, and L. Viennot, "Optimized link state routing protocol for ad hoc networks," *Multi Topic Conference, 2001. IEEE INMIC 2001. Technology for the 21st Century. Proceedings. IEEE International*, pp. 62–68, 2001.
- [8] D.L. Johnson, "Evaluation of a single radio mesh network in south africa," in *ICTD07: International Conference on Information and Communication Technologies and Development*, Bangalore, India, December 2007.
- [9] D.S.J.D. Couto, D. Aguayo, J. Bicket, and R. Morris, "a high-throughput path metric for multi-hop wireless routing," *Wireless Networks*, vol. 11, no. 4, pp. 419–434, 2005.
- [10] "IETF Mobile Ad-Hoc Networks (MANET) Working Group," 1 August 2007, <http://www.ietf.org/html.charters/manet-charter.html>.
- [11] IEEE, *Draft Standard for Information Technology - Telecommunications and Information Exchange Between Systems - LAN/MAN Specific Requirements - Part 11: Wireless Medium Access Control (MAC) and physical layer (PHY) specifications: Amendment: ESS Mesh Networking*, IEEE, New York, NY, USA, March 2007, P802.11s/D1.02.
- [12] A. Tonnesen, "Implementing and extending the optimized link state routing protocol," M.S. thesis, University of Oslo, Norway, 2004.
- [13] H. Lundgren, E. Nordström, and C. Tschudin, "Coping with communication gray zones in IEEE 802.11 b based ad hoc networks," *Proceedings of the 5th ACM international workshop on Wireless mobile multimedia (WOWMOM '02)*, pp. 49–55, 2002.
- [14] K. Xu, M. Gerla, and S. Bae, "Effectiveness of RTS/CTS handshake in IEEE 802.11 based ad hoc networks," *Ad Hoc Network Journal*, vol. 1, no. 1, pp. 107–123, 2003.
- [15] K. Ramachandran, I. Sheriff, E. Belding-Royer, and K. Almeroth, "Routing stability in static wireless mesh networks," *Passive and Active Network Measurement*, vol. 4427, pp. 73–82, June 2007.